



Numerical modeling of reinforced concrete beam using the finite element method

Paulo César de Oliveira Júnior¹, Jerfson Moura Lima², Bruno Rodrigues Amorim³

¹*Programa de pós-graduação em Engenharia Aeroespacial, Universidade Federal do Rio Grande do Norte, paauloz@gmail.com, Natal/RN, Brasil, CEP 59078-970.*

²*Departamento de Engenharia Civil, Universidade de Brasília, jerfsonlima2009@hotmail.com, Brasília/DF, Brasil.*

³*Departamento de Engenharia Civil, Centro Universitário Paraíso, bruno.amorim@fapce.edu.br, Juazeiro do Norte/CE, Brasil.*

Abstract

With the technological advancement of computers and the development of the Finite Element Method, numerous studies have been developed to understand the behavior of structural elements made with concrete. In general, these studies are carried out based on experimental tests. However, numerical modeling has established itself as an efficient tool in the analysis of the behavior of structural elements of reinforced concrete, as it does not demand much time or costs, as it happens in experimental tests, in addition to offering a detailed and punctual investigation of the models analyzed. Therefore, this work aims to develop a non-linear three-dimensional numerical model, using the ABAQUS ® software, capable of simulating the behavior of a reinforced concrete beam using the Finite Element Method. The constitutive models Concrete Damaged Plasticity and Von Mises were used to model concrete and steel, respectively. For model calibration and validation, Gomes [8] experimental work was used. The developed numerical model proved to be suitable for simulating the behavior of reinforced concrete beams.

Keywords: Constitutive Models, Concrete Damaged Plasticity, Von Mises, Non-linear Analysis, Beam, ABAQUS ®.

1. INTRODUCTION

Any mechanical system when subjected to some loading, be it static, dynamic or thermal in nature, will present an answer. However, provides this mechanical system it makes the analysis too complex, since it is linked to the constitutive law of the material that makes up are elements in question [16].

The analysis of efforts and displacements in reinforced concrete structures has the purpose of mathematically reproducing the behavior of the material. In classical

assumptions, a linear relationship between stresses and strains is assumed. The elastic-linear models admit, among other factors, the superposition of effects, where geometric non-linearity can be assumed. However, one must question the validity of such hypotheses for reinforced concrete [19].

The concrete has a behavior that deviates from the elastic-linear hypothesis. When compressed, it exhibits a non-linear behavior under high stresses. In traction, even at relatively low stress levels, concrete presents cracking, which implies a considerable loss of structures stiffness [5].

The non-linearity of the concrete is due to the cracking process, which degrades the material for a loading, thus, the permanent plastic deformation of concrete at least in the early stages, is a result of the degradation of stiffness [13].

The difficulties in computational modeling of reinforced concrete are due to the significant difference between the tensile and compressive strengths of concrete, the non-linearity of the stress-strain relationship even for low stress levels, the creep and shrinkage phenomena that depend on moisture, ambient temperature, the dimensions of the structural elements, the cracking of the concrete and the transmission of forces through the cracks [4].

In the analysis of non-linear structures of reinforced concrete, using the Finite Element Method (FEM), there is great difficulty in characterizing material properties. Thus, many researches have already been carried out in order to develop a model that is as close to reality as possible, managing to predict the behavior of the structure when loading [14].

Thus, a better modeling of reinforced concrete beams should be based on criteria that take into account the damage to reinforced concrete. However, the mathematical systems generated from the formulation of this non-linear problem cannot be solved analytically, but numerically, and these numerical solutions require the application of computational routines [19].

In this sense, the technological advancement of computers and the development of Finite Element Method, together with the non-linearity of the problem and models that best describe the behavior of the material, made possible the computational analysis more closely structures of reality [14].

According to Sanches Junior [19], the modeling of the behavior in service of reinforced concrete, using the Finite Element Method and the application of physical non-linearity, can be realized to in two ways:

- modeling of the relationships between the stresses and strains of the constituent materials, in this case concrete and steel;
- modeling by way of moment-curvature diagrams of a cross section.

1.1. Background

The traditional analysis of concrete structures is based on laboratory tests. In this type of study, the results are limited, considering only a few points of the element, and sometimes these data are difficult to interpret. In this sense, it is necessary to develop mathematical models to complete the experimental analysis and make it possible to generalize the results for different structures and forms of loading [4].

According to Ellobody and Young [7], numerical modeling has established itself as an efficient tool for studying the behavior of concrete structures, as it does not generate large costs and does not require a lot of time, as occurs with experimental tests. This stems from the fact that there is no need for waiting time for curing the concrete or even extra expenses with materials for the execution and testing of the structures. In addition, it offers a thorough and punctual

investigation of the models, enabling a broader and more complete analysis.

From the validation of a numerical model as a model that can realistically represent the behavior of a structure, it is possible to carry out a series of analyzes by varying the geometric characteristics of the computational model for example, developing new models that will also present results close to reality.

The numerical simulation is still in an important academic tool to, especially in the case of limited laboratory environment, and to allow the analysis of structures from the validated models of experimental work and are widely disseminated in academia. Thus, several studies in different types of structures can be realized without the direct need for a laboratory of engineering.

1.2. Objectives

The main objective of this work is to develop a non-linear three-dimensional numerical model using the Finite Element Method, using the ABAQUS ® software, capable of simulating the behavior of a reinforced concrete beam.

1.2.1. Specific Objectives

The specific objectives are:

- implementation of the numerical model of reinforced concrete beam in the ABAQUS ® software;
- comparison of the numerical results obtained with the experimental results verified by Gomes [8];
- evaluate the efficiency of the concrete damaged plasticity constitutive model for the simulation of concrete behavior;
- to study the stresses acting on the structure during the loading process.

2. EXPERIMENTAL/MATERIALS AND METHODS

The numerical model was calibrated and validated from the experimental tests performed by Gomes [8], by means of a comparison between the experimental and numerical results for the load-displacement relationship. For the development and simulation of numerical models, the ABAQUS ® software as used. The constitutive models Concrete Damaged Plasticity and Von Mises were used to model concrete and steel, respectively.

2.1. Experimental Model Analyzed

In this experimental program Gomes [8] studied four beams: a reference beam (V_0) in reinforced concrete and three beams ($V_{0.5}$, $V_{0.8}$, $V_{1.0}$) reinforced by shearing with steel fibers. This study refers to an experimental analysis of the efficiency of steel fibers in reinforcing the shear of reinforced concrete beams. In this work was analyzed only the reference beam. According to Gomes [8], it was opted for a non-uniform distribution for the transversal reinforcement, for the definition of a region of analysis in his experimental program. The Figure 1 shows a longitudinal section of the beam with all units in millimeters.

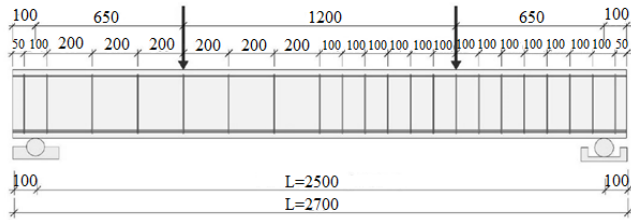


Figure 1. Longitudinal view of the modeled beam. Adapted from [8].

The Figure 2 shows the cross section of the beam with all dimensions in millimeters.

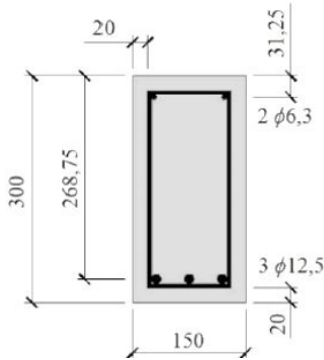


Figure 2. Cross section of the beam studied [8].

The beam was subjected to the four points bending test, also called the Stuttgart test, whose loading scheme is illustrated in Figure 3. The instrument for reading the vertical displacements of the beam, the Linear Variable Differential Transformer (LVDT), was fixed by means of a device known as Yoke. The load was applied manually by means of a hydraulic pump with a capacity of 10^3 kN.

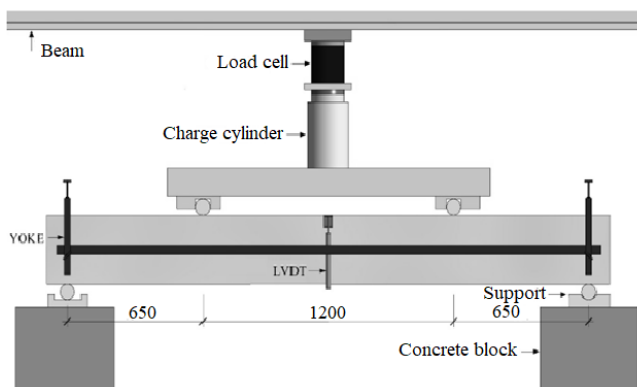


Figure 3. Experimental test system Adapted from [8].

2.2. Computational Program Used

The ABAQUS ® software is established and has already been validated for many complex conditions, providing facilities through several modules, allowing to analyze the effects under study.

As Alelvan [3] to complete this analysis software consists of the steps of pre-processing, simulation and post-processing, which are described below:

1. in the first step, the entire physical problem is portrayed, defining the geometry, the materials, the sections, the possible interactions, boundary conditions and meshes of elements. The input file can be defined using the ABAQUS/CAE ® module or a text editor;
2. a from the input file is performed solving the numerical problem in the background through the ABAQUS/Explicit ® or ABAQUS/Standard ® module. These modules are differentiated by the way in which the numerical integration is made;
3. the post numerical analysis are generated binary files that are stored in the output database. These files can have their results analyzed, including deformed shape, animations, color graphics and cartesian graphics, using ABAQUS/CAE ® visualization module.

2.3. Constitutive Model of Materials

In numerical modeling, one of the most important characteristics is the constitutive model of the materials used, in order to describe their real behavior and thus promote a more precise analysis.

2.3.1. Concrete Damaged Plasticity

There is a large number of constitutive models that describe the behavior of concrete when subjected to loads, which do simulation with the consideration of simplifying hypotheses [15].

The Concrete Damaged Plasticity (CPD) is based on the assumption damage scalar (isotropic), being indicated for cases in which the concrete element is subjected to arbitrary loading conditions, including cyclic loading. This model considers the degradation of elastic stiffness induced by plastic deformation, both in traction and in compression. It also describes the behavior of concrete in relation to the effects of stiffness after recovery under cyclic loading [9].

The CDP model was developed by Lubliner *et al.* [13] and modified by Lee and Fenves [11] based on the plasticity and mechanics of the damage. Subsequently, Alfarah, López-Almansa and Oller [2] presented a new methodology to calculate the evolution of the damage variables.

The model proposed by Lubliner *et al.* [13], also known as the Barcelona model, considers that the plastic deformation represents all irreversible deformations, even those caused by cracking. However, Lee and Fenves [11] seek to adapt the model to concrete behavior submitted to cyclic loading, whereas the former does not it had suitable for conducting

such analyzes, so it is proposed to use two variables damage plastic, one for traction (d_t) and one for compression (d_c) [9].

The behavior of concrete is dependent on four constitutive plastic parameters: the form factor (K_c), the expansion angle φ , the relationship between the compressive strength of biaxial and uniaxial concrete f_{b0}/f_{c0} and the potential plastic eccentricity (ϵ). They define the potential non-associative plastic flow rule in the plastic damage model (LIMA, 2018). Thus, the plastic parameters are responsible for the expansion of the equations of material behavior in uniaxial state to the multiaxial state [1]. In their research, Alfara, López-Almansa and Oller [2] assumed the values present in Table 1 for the plastic parameters.

Table 1. Plastic parameters [2].

K_c	φ	f_{b0}/f_{c0}	ϵ	μ
0,7	13°	1,16	0,1	0

In Concrete Damaged Plasticity the elastic and plastic deformations are determined independently and are then added together to obtain the total deformation. The elastic deformations are only a function of the modulus of elasticity and the Poisson's ratio, whereas the plastic deformations are obtained from the stress-strain curve [1].

Axial deformations in compression can be decomposed into crush deformation (inelastic) (ϵ_c^{ch}), undamaged elastic deformation (ϵ_{0c}^{el}), plastic deformation (ϵ_c^{pl}) and damaged elastic deformation (ϵ_c^{el}) [2].

The characteristic strength of concrete (f_{ck}) and the secant elasticity modulus (E_0) can be obtained from the equations established by fib Model Code 2010 [10] through the data of average compressive strength (f_{cm}) and the modulus of initial elasticity (E_{ci}):

$$f_{cm} = f_{ck} + 8 \quad (1)$$

$$E_{ci} = 10000 \cdot f_{cm}^{\frac{1}{3}} \quad (2)$$

$$E_0 = \left(0,8 + 0,2 \cdot \frac{f_{cm}}{88} \right) \cdot E_{ci} \quad (3)$$

The uniaxial behavior of concrete under compression (Figure 4) has three stages, each of which describes one aspect of the material behavior when subjected to one charge.

The first stage has a linear elastic behavior. In the second stage the cracks would start to increase in quantity, length and opening. Thus, the fracture of the concrete start, at first, due to the formation of cracks next to the aggregates. With the significant increase in cracks, the non-linearity of the material would be evident, but they would still be considered stable. Finally, in the third stage, when exceeding this limit, even if the load remained constant, the cracks would continue to

propagate, starting the micro cracking of the matrix with the formation of internal micro cracked zones [9].

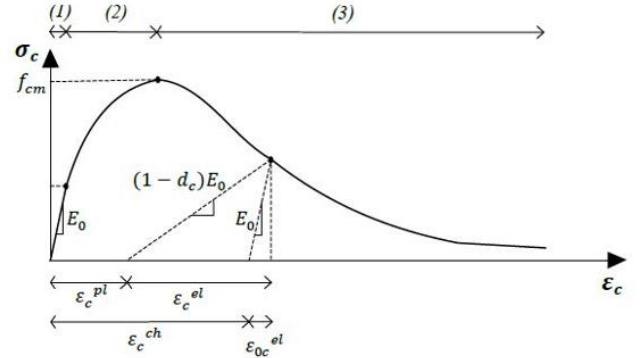


Figure 4. Uniaxial behavior of concrete under compression [12].

According to fib Model Code 2010 [10] *apud* Lima [12] the first stretch extends to the tension of $0,4f_{cm}$ and is a linear, the second goes from $0,4f_{cm}$ to f_{cm} and the third is the stretch of softening. Each of these stages is described by an equation:

First section

$$\sigma_{c(1)} = E_0 \cdot \epsilon_c \quad (4)$$

Second section

$$\sigma_{c(2)} = \frac{E_{ci} \frac{\epsilon_c}{f_{cm}} - \left(\frac{\epsilon_c}{\epsilon_{cm}} \right)^2}{1 + \left(E_{ci} \frac{\epsilon_{cm}}{f_{cm}} - 2 \right) \frac{\epsilon_c}{\epsilon_{cm}}} \quad (5)$$

Third section

$$\sigma_{c(3)} = \left(\frac{2 + \gamma_c f_{cm} \epsilon_{cm}}{2 f_{cm}} - \gamma_c \epsilon_c + \frac{\epsilon_c^2 \gamma_c}{2 \epsilon_{cm}} \right)^{-1} \quad (6)$$

$$\gamma_c = \frac{\pi^2 f_{cm} \epsilon_{cm}}{2 \left[\frac{G_{ch}}{l_{eq}} - 0,5 f_{cm} \left(\epsilon_{cm} (1 - b) + b \frac{f_{cm}}{E_0} \right) \right]^2} \quad (7)$$

$$b = \frac{\epsilon_c^{pl}}{\epsilon_c^{ch}} \quad (8)$$

The equivalent length of the finite element (l_{eq}) depends on the mesh size, the type of element used and the crack direction, but it can be determined by the relationship between the volume and the area of the largest surface area of the finite element. Based on experimental observations, $b=0,9$ is initially adopted. In this way, the stress-strain curve is obtained and, with that, an average value of b . Thus, an interactive calculation is performed until a convergence is defined [2].

According to Qureshi, Lam and Ye [17] *apud* Lima [12], three different paths can be taken to define softening in traction. The first consists of a linear approach, that is, after reaching the maximum tensile strength, the drop in strength, in relation to the crack opening, occurs in a linear manner (Figure 5-a). In the second, a little more detailed behavior is adopted, so that a bi-linear function is assumed for the loss of resistance (Figure 5-b). The third and last path (Figure 5-c), consists of a more realistic method, defined by an exponential expression proposed by Cornellissen, Hordijk and Reinhardt [6] *apud* Lima [12].

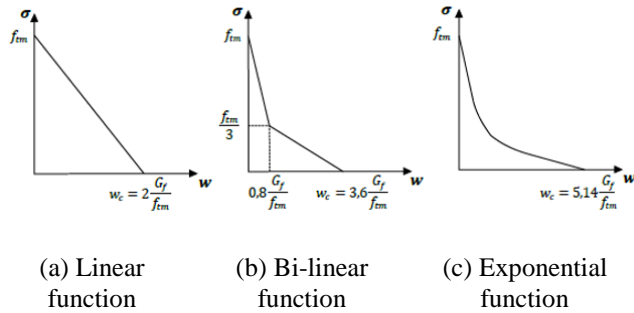


Figure 5. Softening in the traction in relation to the crack opening [12].

According to fib Model Code 2010 [10] *apud* Lima [12], the values of mean tensile strength (f_{tm}) and fracture energy (G_f) are defined according to the equations:

$$f_{tm} = 0,3016 f_{ck}^{2/3} \quad (9)$$

$$G_f = 0,073 f_{cm}^{0.18} \quad (10)$$

According to Oller [15] *apud* Lima [12] energy for crushing concrete (G_{ch}) can be obtained by equation (11):

$$G_{ch} = \left(\frac{f_{cm}}{f_{tm}} \right)^2 G_f \quad (11)$$

Cornellissen, Hordijk and Reinhardt [6] relate the stress to the crack opening through an exponential expression, equation (12), assigning $c_1=3$ and $c_2=6,93$. In addition, it establishes the critical crack (w_c) opening according to equation (13):

$$\frac{\sigma_t(w)}{f_{tm}} = \left[1 + \left(c_1 \frac{w}{w_c} \right)^3 \right] e^{-c_2 \frac{w}{w_c}} - \frac{w}{w_c} (1 + c_1^3) e^{-c_2} \quad (12)$$

$$w_c = 5,14 \frac{G_f}{f_{tm}} \quad (13)$$

According to Alfarah, López-Almansa and Oller [2] *apud* Lima [12] the strain values that define the second stretch of the stress-strain curve can be obtained using equation (14),

with ϵ_{tm} being the strain corresponding to average tensile strength:

$$\epsilon_t = \epsilon_{tm} + \frac{w}{l_{eq}} \quad (14)$$

A Figure 6 shows the uniaxial behavior of the concrete to the traction.

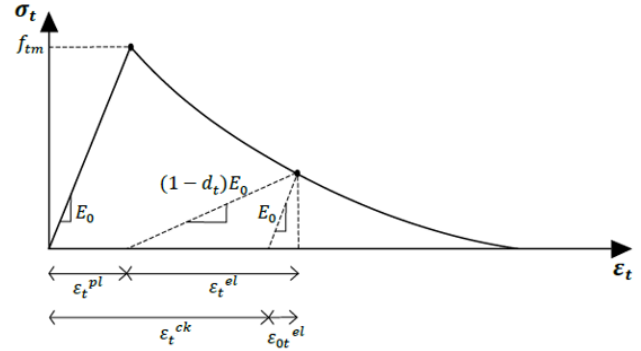


Figure 6. Uniaxial behavior of concrete under tension [12].

Analogous to the compression deformations, the axial deformations in the traction (ϵ_t) can be decomposed in: crack deformation (inelastic) (ϵ_t^{ck}), undamaged elastic deformation (ϵ_{0t}^{el}), plastic deformation (ϵ_t^{pl}) and damaged elastic deformation (ϵ_t^{el}).

2.3.2. Behavior of Steel

Steel has an elastic-plastic constitutive model, with isotropic flow. Thus, the response is obtained regardless of the strain rate. The axial behavior for steel, required by the constitutive Von Mises model can be defined by the bi-linear (Figure 7) or tri-linear (Figure 8) [12].

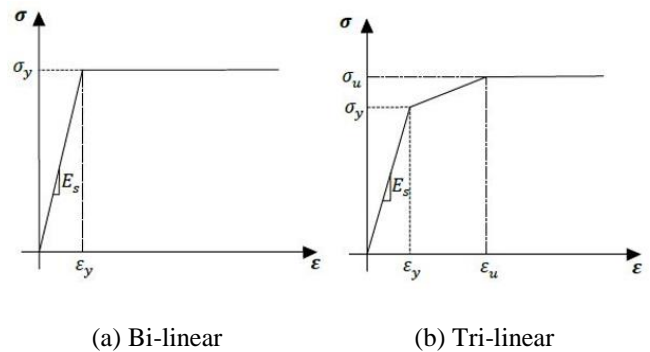


Figure 7. Uniaxial behavior of steel [12].

The first part of the bi-linear curve is linear elastic, which extends until the yield stress of the material is reached. The second is a plastic region, where the stress remains constant

with only variation in the deformation. The bi-linear model establishes the perfectly elastic-plastic behavior. In the tri-linear curve, the behavior is initially elastic, followed by a hardening and immediately afterwards it presents a perfectly plastic flow [12].

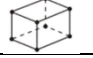
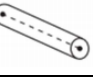
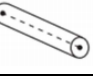
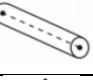

3. RESULTS AND DISCUSSION

The process of implementing the model in the software until its calibration included several steps.

3.1. Modeling Elements

The elements of the computational model were defined based on the constituent elements and geometric characteristics of the reference beam of Gomes [8]. In addition, a plate (150mmx150mm and 20mm thick) was inserted for the support and load application regions of the bending test, just to carry out the load transmission to the beam. For each component of the beam studied, the type of element was defined in ABAQUS ® according to Table 2.

Table 2. Elements of modeling.

Element	Spatial dim.	Form	Finite elem.	N° of nodes	Illustration [20]
Concrete beam	3D	Solid	C3D8R	8	
Long. Armature (ø12,5mm)	2D	Wire - Truss	T3D2	2	
Long. Armature (ø6,3mm)	2D	Wire - Truss	T3D2	2	
Stirrup (ø4,2mm)	2D	Wire - Truss	T3D2	2	
Plate	3D	Solid	C3D8R	8	

3.2. Materials Constitutive Model

For each group of elements (concrete beam, steel bars and plate), the constitutive model was defined to describe its adequate behavior in the case of the performance of efforts in the structure.

3.2.1. Concrete

The concrete behavior was described using Concrete Damaged Plasticity, which is implemented in ABAQUS ®. It should be noted that the study only contemplates static loading according to the model by Lubliner *et al.* [13], so that the parameters of damage to traction and compression implemented by Lee and Fenves [11] were not considered for analyzes with cyclic loads.

When using the damage-plastic model, the data on average compressive strength (f_{cm}) and its respective deformation (ϵ_{fcm}) (Table 3) were used, defined by Gomes [8] through the axial compression test of concrete.

Table 3. Values of tension and deformation of concrete of the reference beam. Adapted from [8].

f_{cm} (MPa)	ϵ_{fcm} (‰)
26,89	1,88

In Table 4 are checked the parameters used for concrete in this work. In the plastic parameters, there was an adaptation of the dilation angle, as it presents a better response for the model during its calibration.

Table 4. Parameters for concrete.

Modulus of elasticity (GPa)	Poisson's Ratio	Parameter's plastics
25,79	0,2	$\varphi=10^\circ$
		$\epsilon=0,1$
		$f_{bo}/f_{co}=1,16$
		$K_c=0,7$
		$\mu=0$

3.2.2. Steel

In this work, the elastic-plastic constitutive model was used to simulate the mechanical behavior of the reinforcement in concrete. The uniaxial behavior implemented in the model considered of the bi-linear stress-strain relationship. Thus, the Elastic and Plastic models available in the ABAQUS ® material library were used. The mechanical properties of steel bars were determined by Gomes [8] from the uniaxial tensile test. Table 5 show the yield stress values (f_{sy}), rupture stress (f_{su}) and their respective strain values ϵ_{sy} and ϵ_u .

Table 5. Mechanical properties of reinforcement. Adapted from [8].

D. (mm)	f_{sy} (MPa)	ϵ_{sy} (‰)	f_{su} (MPa)	ϵ_u (‰)	E_s (GPa)	Poisson
ø4,2	609,5	3,02	672,3	10	201,5	0,3
ø6,3	568,5	2,15	610,2	8,5	264,9	0,3
ø12,5	610,3	3,05	716,0	10	200,1	0,3

3.2.3. Plate

The plates used in the regions of support and load application relating to test Stuttgart were defined as highly rigid elements to avoid damage to the beam concrete reinforced due to the direct application of point charge in the simulation, thus the plates do not they must deform, but only transmit the stress to the structure.

3.3. Contour and Loading Conditions

In the support conditions of the computational model (Figure 8), the same restrictions present in the experimental work were used. Both supports were defined in line on the

applied plate, one of the first gender with two displacement restrictions ($U_x=U_y=0$) and the other of second gender with three displacement restrictions ($U_x=U_y=U_z=0$). To describe the four-point bending test in the computational model, point loads were applied at two points and on the plate (Figure 8), each 650mm away from the supports, also according to the experimental model.

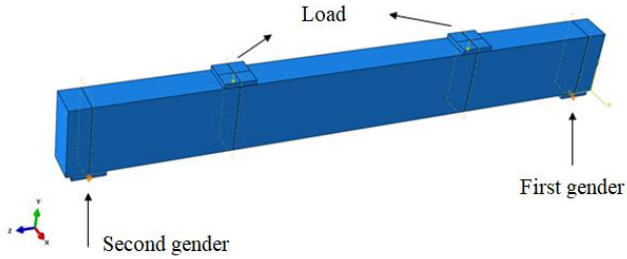


Figure 8. Support conditions and load application.

The point load was defined in the Load module of ABAQUS ® and in the Step module the type of Static analysis, Riks, to obtain the correct non-linear equilibrium paths. The initial increment established was 100N.

3.4. Interactions

The numerical model is formed by different parts that interact with each other. For the consideration of the non-linearity of contact between the elements of the simulation, ABAQUS ® makes it possible to define the interaction between the elements of the simulation in its Interaction module.

To simulate the contact between the plates and the horizontal surfaces of the top and bottom of the beam (Figure 9), a restriction offered by ABAQUS ® called Tie was used. According Rojas [18], this type of interaction considers that there is no relative displacement between the nodes of the slave surface to the master surface, generating a seamless transfer of tensions.

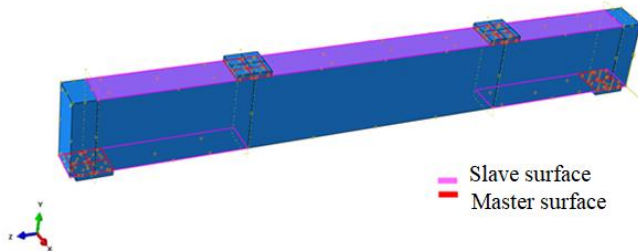


Figure 9. Plate-concrete contact.

For the longitudinal and transverse reinforcement (Figure 10), the Embedded Region constraint type, also present in the software, was defined. This type of contact simulates the perfect adhesion between the materials, that is, there is no slipping of the bars. Thus, the elements that are involved (Embedded Region) are determined, in this case the reinforcements, and the component that involves (Host Region), the concrete beam.

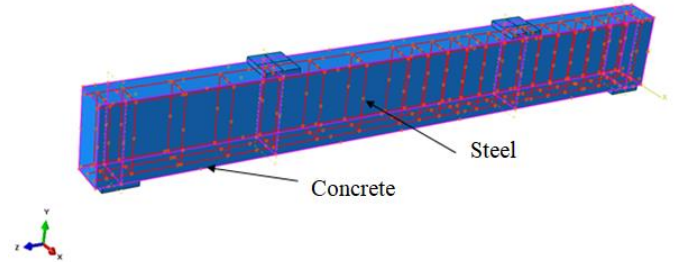


Figure 10. Reinforcements embedded in concrete.

3.5. Mesh

The choice of mesh for concrete influences the calculated values of stress and strain using the damage-plastic model. Table 6 shows the meshes defined for the beam constituent elements.

Table 6. Finite element characteristics.

Element	Interpolation order	Finite Element	Size (mm)
Beam	Quadratic	C3D8R	20
Long. Reinf. (ø12,5mm)	Linear	T3D2	5
Long. Reinf. (ø6,3mm)	Linear	T3D2	5
Stirrup (ø4,2mm)	Linear	T3D2	5
Plate	Quadratic	C3D8R	30

3.6. Calibration of the Number Model

The computational model was calibrated by comparing the load-displacement curve of the simulation with the reference beam tested by Gomes [8]. Thus, the values must be extracted at coincident points in the simulation and in the experimental test with a system as shown in Figure 11.

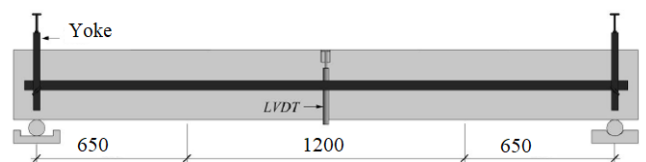


Figure 11. Displacement monitoring [8].

In the development of mathematical models has been observed that the use of an angle of dilatancy 10° resulted in a better approximation with the experimental result, although Alfarah, López-Almansa and Oller [2] recommend 13° . Figure 12 shows the comparison between the experimental and numerical result.

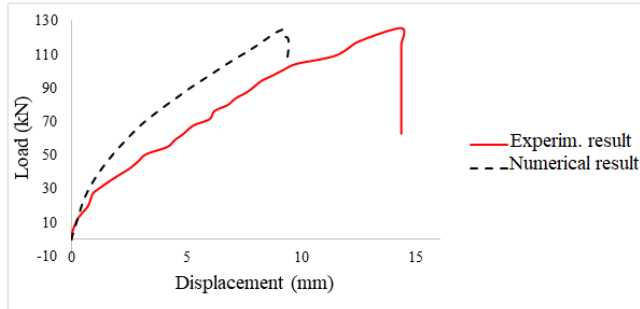


Figure 12. Force-displacement curve used in model calibration.

The simulation presented results close to those found in the experimental test of flexion at four points, with very similar values for the ultimate load of the beam (V_u) according to Table 7, with an error of 0,45% for this one. The numerical load-displacement curve was more rigid than the experimental one, since with respect to be displacement related to the ruin load (δu) there was a greater divergence between the results.

Table 7. Ruin load and displacement of the numerical and experimental result.

Result	V_u (kN)	δu (mm)
Experimental	125,50	14,32
Numeric	124,93	9,18

The factor that causes the greatest stiffness of the numerical curve is probably in the stress-strain relationship, which were modeled according to the theoretical curves proposed by previous research and data obtained in experimental tests. In addition, in the computational model an interaction was used that simulates the perfect adhesion between the concrete and the reinforcement, which does not occur in practice.

3.7. Complementary Analysis of the Numerical Model

With the computational model representing the behavior of the experimental model, it is possible to carry out several structural analyzes. In this work, the flexural reinforcement and cracking of the beam by Gomes [8] were further studied.

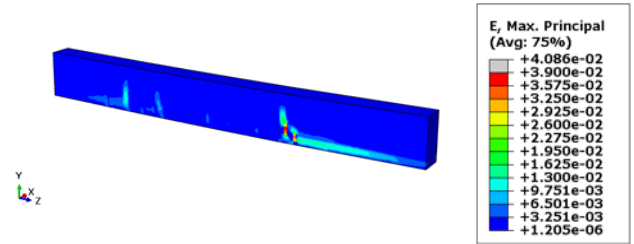
3.7.1. Analysis of the Mapped Fissure

During the flexion test, Gomes [8] performed the crack mapping (Figure 13-a), so that these results can also use for

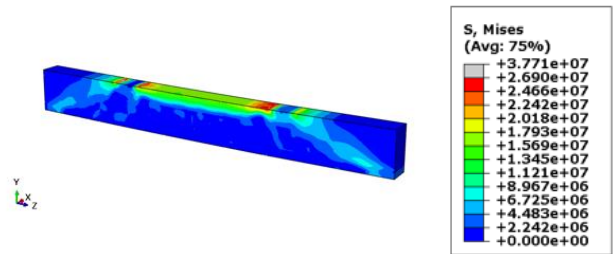
comparative analysis of the experimental study with the simulation performed in ABAQUS®.



(a) Crack mapping [8]



(b) Deformation verified in ABAQUS®



(c) Tension verified in ABAQUS®

Figure 13. Development of deformations and stress in the mapped crack.

Through the analysis of the deformations developed in the numerical model it is possible to perceive where the cracked regions are. The numerical result is in accordance with the crack mapping carried out in the experimental work, also showing higher values of deformation in the region with greater stirrup spacing (Figure 13-b). In addition, the modeling allows to perceive the development of stresses in the beam (Figure 13-c), which occur with greater intensity in the region with the greatest cracking.

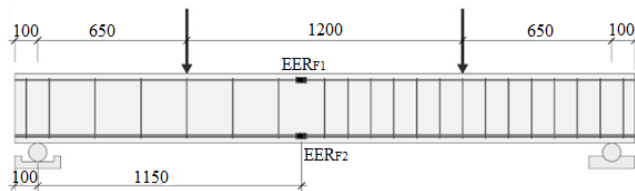
With the analysis of the stress and strain distributions in the numerical model, it is observed that it can simulate the rupture mode of the experimental model. In general, it is noted that the beam presents a characteristic shear rupture mode, with the formation of a crack of approximately 45° , originating in the support and that invades the region compressed by the flexion.

3.7.2. Flexural Armor Analysis

From the validation of the computational model, the longitudinal reinforcement of the beam was analyzed. Similar

to the load-displacement curve of the concrete beam, the longitudinal reinforcement was also analyzed according to the points verified in the experimental work.

According to Gomes [8], for the instrumentation of the flexural reinforcements, Electric Resistance Extensometers (EER) were installed in two points of the structure to record the deformations (Figure 14). It is observed that the EER_{F1} is promoting the analysis in terms of compression and the EER_{F2} in terms of traction.



(a) Identification of points



(b) Instrumented section

Figure 14. Flexural reinforcement. Adapted from [8].

The comparison between the experimental and numerical results is seen in Figure 15, which also shows the steel deformation value (ϵ_{sy}) of the flexural reinforcement ($\phi 12,5\text{mm}$) in the tensile region, and the strain value referring to the average strength of the concrete (ϵ_{fcm}) in the compression region.

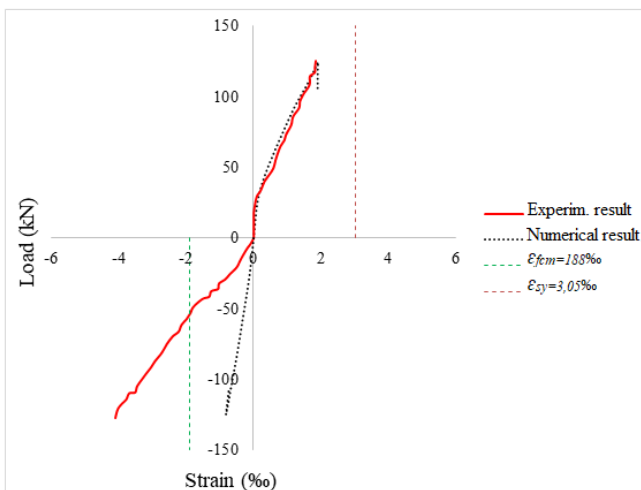


Figure 15. Numerical and experimental load strain.

It is observed that there was a considerable divergence between the experimental and the numerical model for the load-strain ratio of the flexural reinforcement subjected to compression. Table 8 shows the ultimate strain values (ϵ_u) found for compression and tension.

Table 8. Ultimate strain for the flexural reinforcement subjected to compression and traction.

Analyze	ϵ_{cu} (‰)	ϵ_{tu} (‰)
Experimental	4,08	1,87
Numeric	0,81	1,94

However, according to Gomes (2016), it is likely that the record of compression strains of the reference beam (V_0) is incorrect, since the angular constant (k_c) for the compression reinforcement was very different from the values found for the other tested beams ($V_{0,5}$, $V_{0,8}$, $V_{1,0}$). No experimental work (Table 9). This constant evaluates the tangent of the inclination angle of the linear portion of the load-strain relationship for compressed longitudinal reinforcement.

Table 9. Parameters that define the load-strain relationship. Adapted from [8].

Beam	k_c
V_0 – Reference	40,03
$V_{0,5}$	141,09
$V_{0,8}$	109,75
$V_{1,0}$	136,48

In addition, in the analysis of the numerical result of deformation of the compression reinforcement, we have $\epsilon_{cu} = 0,81\% < \epsilon_{fcm} = 1,88\%$, which is more consistent with the failure mode of the reference beam (shear), not crushing of the concrete was verified after the experimental test.

4. CONCLUSION

The developed numerical model provides approximate results to the experimental ones, although the numerical load-displacement curve has been shown to be a little more rigid, the result of the ruin load was very similar to the real one, with the same behavior of the longitudinal tensile reinforcement being verified and in beam break mode.

The divergence found for the load-deformation curves of the longitudinal compression reinforcement is mainly explained by the error verified in the experimental work, because it is a region of poor adhesion and by the very difficult of the extensometers in capturing an ideal behavior in the compression region. Although the numerical result of load-deformation for compression reinforcement is more consistent with beam breaking mode, it is not possible to say that this curve defines the correct behavior.

The simulation developed contributed to a better understanding of the behavior of the reinforced concrete beam during the loading process, being verified how the stresses deformations act in the formation of cracks.

Although the study contemplates only the points analyzed in the experimental work, the simulation allows a thorough analysis of all the constituent points of the beam, making it possible to carry out a more complete analysis of the loading process in the structure.

For all these reasons, it is concluded that the main objective of this work was achieved, since the numerical model developed was able to represent the real behavior of the reinforced concrete beam.

ACKNOWLEDGEMENTS

The first author would like to thank Universidade Federal do Rio Grande do Norte (UFRN) for all the support given. The second author would like to thank Universidade de Brasília (UnB). The third author would like to thank the Centro Universitário Paraíso (UniFAP).

REFERENCES

- [1] AGUIAR, O. P. Estudo do comportamento de conectores Crestbond em pilares mistos tubulares preenchidos com concreto. PhD dissertation. Universidade Federal de Minas Gerais: Escola de Engenharia, Belo Horizonte, 2015.
- [2] ALFARAH, B.; LÓPEZ-ALMANSA, F.; OLLER, S. New methodology for calculating damage variables evolution in Plastic Damage Model for RC structures. *Engineering Structures*, v. 132, n. January, p. 70–86, 2017.
- [3] ALELVAN; G. M. Aplicação do método dos elementos finitos para análise de deslizamentos de encostas e impacto em barreiras. PhD dissertation. Universidade de Brasília: Faculdade de tecnologia, Brasília, 2017.
- [4] AURICH, M. Simulação computacional do comportamento do concreto nas primeiras idades. PhD dissertation. Escola Politécnica da Universidade de São Paulo: Departamento de Engenharia de Estruturas e Geotécnica, São Paulo, 2008.
- [5] BANDINI, P. A. C. A consideração da não-linearidade física no cálculo de flecha em vigas de concreto armado. PhD dissertation: Universidade Estadual de Campinas: Faculdade de Engenharia Civil, Arquitetura e Urbanismo, Campinas, 2015.
- [6] CORNELLISSSEN, H.; HORDIJK, D.; REINHARDT, H. Experimental determination of crack softening characteristics of normal weight and lightweight concrete. *Heron*, v. 31, n. 2, p. 45–56, 1986.
- [7] ELLOBODY, E.; YOUNG, B. Performance of shear connection in composite beams with profiled steel sheeting. *Journal of Constructional Steel Research*, v. 62, n. 7, p. 682–694, 85, 2006.
- [8] GOMES, L. D. S. Análise experimental da eficiência das fibras de aço no reforço ao cisalhamento de vigas em concreto armado. PhD dissertation. Universidade Federal do Pará: Instituto de Tecnologia, Programa de Pós-Graduação em Engenharia Civil, Belém, 2016.
- [9] GUERRA, M. B. B. F. Modelos de concepção para estruturas em concreto armado com comportamento não linear obtidos pelo método de bielas e tirantes e otimização topológica. PhD dissertation. Universidade Federal de Minas Gerais: Escola de Engenharia, Belo Horizonte, 2017.
- [10] INTERNATIONAL FEDERATION STRUCTURAL CONCRETE. fib-MC2010 (2012). The International Federation for Structural Concrete, fib Model Code 2010 Final draft. Volume 2, April 2012.
- [11] LEE, J. H.; FENVES, G. L. Plastic-damage model for cyclic loading of concrete structures. *J. Eng. Mech. (ASCE)*, v. 124, n. 8, p. 892–900, 1998.
- [12] LIMA, J. M. Estudo da capacidade resistente do conector de cisalhamento treliçado via método dos elementos finitos. PhD dissertation. Universidade de Brasília: Faculdade de Tecnologia, Departamento de Engenharia Civil e Ambiental, Brasília, 2018.
- [13] LUBLINER, J.; OLIVER, J.; OLLER, S.; OÑATE, E. A plastic-damage model for concrete. *International Journal of Solids and Structures*, v. 25, n. 3, p. 299–326, 1989.
- [14] LYRA, P. H. C. Modelagem numérica de estruturas de concreto armado utilizando o programa Atena. PhD dissertation. Escola Politécnica da Universidade de São Paulo: Departamento de Engenharia de Estruturas e Geotécnica, São Paulo, 2011.
- [15] OLLER, S. (1988). Un modelo de "daño continuo" para materiales-friccionales. Trabajo para grado de Doctor, Escola Tècnica Superior D'Enginyers De Camins, Canals I Ports, Universitat Politècnica de Catalunya, Barcelona, p. 471.
- [16] PEREIRA JUNIOR, W. M. Análise numérica de estruturas de concreto com fibras utilizando mecânica do dano. PhD dissertation. Universidade Federal de Goiás: Escola de Engenharia Civil, Goiânia, 2014.
- [17] QURESHI, J.; LAM, D.; YE, J. Effect of shear connector spacing and layout on the shear connector capacity in composite beams. *Journal of Constructional Steel Research*, v. 67, n. 4, p. 706–719, 2011.
- [18] ROJAS, N. R. Análise computacional de vigas reforçadas ao cisalhamento com sistemas EB-FRP: efeitos das interação estribos-fibras. PhD dissertation. Universidade de Brasília: Faculdade de tecnologia, Departamento de Engenharia Civil e Ambiental, 2017.
- [19] SANCHES JUNIOR, F. Cálculo de deslocamentos em pavimentos de edifícios considerando-se modelos próprios para concreto armado. 1998. PhD dissertation. Universidade de São Paulo: Escola de Engenharia de São Carlos, São Carlos, 1998.
- [20] SIMULIA. Abaqus analysis user's manual. USA, 2010.